university of groningen

Effect of WHSV and magnesium impregnation on HZSM-5 catalyst coke formation in MTA-process

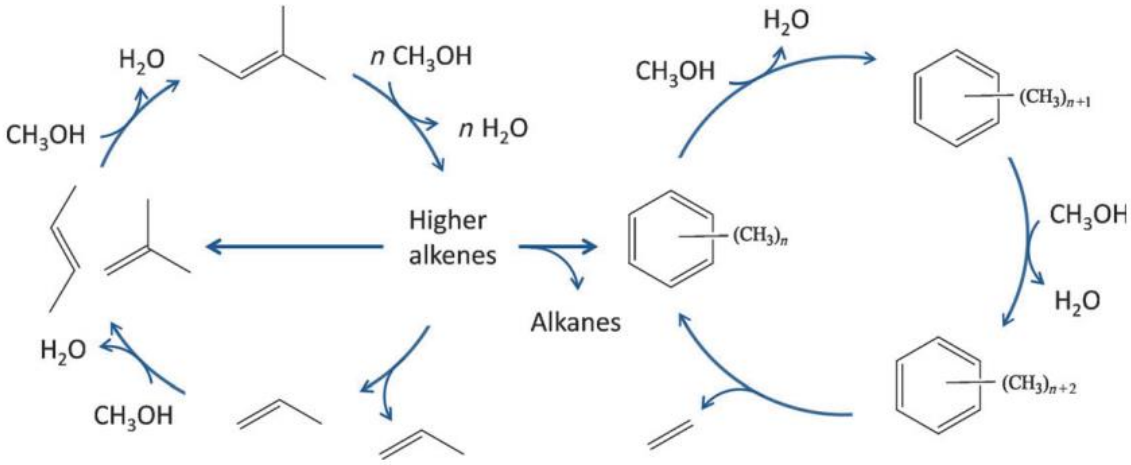

(Olsbye et al., 2012)

Name: Mark Eling
Student number: S3696847
Supervisor: Dr. Ir. Jingxiu Xie
Second supervisor: Prof. dr. Jun Yue
Date: 16-05-2021

Contents

Abstract

In this project, the effect of weight hour space velocity (WHSV) and magnesium impregnation on coke formation during methanol to aromatics (MTA) reaction was investigated. Nitrogen was used as carrier gas in combination with a methanol saturator to lead this gas mixture through a packed-bed reactor. A HZSM-5 catalyst was used in the reactor. The effect of WHSV on coke formation was analysed by changing the amount of catalyst. Magnesium was impregnated in the HZSM-5 catalyst via incipient wetness impregnation with different weight percentages of magnesium. The impregnated catalyst was analysed with XRD, nitrogen physisorption and NH_3-TPD. It was found that magnesium impregnation does not affect the crystalline structure but decreases the acidity of the catalyst. Product analysis showed that methane has the highest selectivity of the formed gas products and increases at larger WHSV. It seemed that methane formation is favoured when the catalyst is deactivated. The spent catalyst is analysed with thermogravimetric analysis (TGA). The TGA data shows that decreasing the WHSV decreases coke formation, while magnesium impregnation increases coke formation. The reason for this is higher amounts of catalyst decreases the average coke formation and that lower acidity leads to carbon build-up, which is responsible for coke formation.

Introduction

The use of fossil feedstocks has several disadvantages. The main disadvantages of fossil resources for the future are depletion of fossil resources and their negative effect on the environment (He et al., 2021). It has been found that methanol is a good alternative for synthesizing aromatics and low olefins without using oil (Zhu et al., 2019). An important methanol process is the methanol to aromatics process (MTA), which discovered by Mobil in 1976. This process is part of a general group ,which is called the methanol to hydrocarbons (MTH) reaction (Li et al., 2021). The importance of this group of reactions lies in the absence of petroleum resources, as mentioned before. Besides methanol to aromatics (MTA), also methanol to olefins (MTO), methanol to propylene (MTP) and methanol to gasoline (MTG) are all processes that are part of the general methanol to hydrocarbon reactions (Li et al., 2021). All the produced chemicals, aromatics, olefins, propylene, and gasoline are important (intermediate) compounds in the chemical industry.

Because the mechanism of the MTA-process is complex with multiple reaction steps involved, it is accepted that the dual cycle hydrocarbon pool is the mechanism involved (Pinilla-Herrero et al., 2018). The dual cycle hydrocarbon pool is a mechanism in which alkenes and aromatics are used as intermediates between two inter-related cycles. In this mechanism several reactions are involved, such as cracking, methylation, dealkylation cyclization and hydrogen transfer. At the acid sites of the catalyst, methanol is dehydrated and then converted to alkenes, via the reactions mentioned before (Li et al., 2021). The formed olefins could be converted to aromatics in two different ways. In the first way olefins are converted to aromatics via hydrogen transfer reaction. In these reactions, alkanes are formed as a side product. The second way to form aromatics from olefins is with the dehydrogenation reaction. In this reaction hydrogen is formed. Due to formation of too large molecules deactivation of the catalyst occurs (Pinilla-Herrero et al., 2018). The reason for this is that those large molecules cannot diffuse through the pores of the catalyst, which leads to trapping of these molecules. Carbonaceous deposits are formed, which deactivate the catalyst. This trapping, which leads to coke formation, is one of the biggest drawbacks of the MTA-process.

The HZSM-5 catalyst has been widely used as catalyst for the methanol to aromatics reaction (Zhu et al., 2019). The HZSM-5 catalyst used in this project has a SiO_2/Al_2O_3 ratio of 23. The catalyst is obtained from Zeolyst International (product number CB-V2314) (He et al., 2021). The obtained catalyst is converted from the ammonia-form into the H-form by calcination. The samples were consequently pressed and sieved to a final sieve fraction of 300-500 µm. It is demonstrated that modification of the catalyst with metal ions (Ag^+, Zn^{2+},Ga^{2+} and Ni^+) modifies the acidity of the surface area of the catalyst (Li et al., 2021). From other research it is found that modification changes the selectivity of the catalyst in such a way that the hydrogenation reaction is favoured over the hydrogen transfer reaction, so that formation of paraffins is supressed (Pinilla-Herrero et al., 2018).

Based on other research the following could be concluded. Firstly, the unmodified catalyst favours the hydrogen transfer reaction (Zhu et al., 2019). The reason for this is that the hydrogen transfer index (HTI index) is higher than for example the HZSM-5 catalyst which is modified with Zn metal ions. The HTI index is defined as the ratio between C3- and C4-alkanes and C3 and C4-alkenes. The HTI index for the unmodified ZSM-5 catalyst equals 19.18, while the HTI index for the Zn modified HZSM-5 catalyst is between 1.87 and 3.54. The high value for the HTI index indicates that the selectivity for alkanes should be high when the unmodified catalyst is used. Secondly, methane is formed in the MTA-reaction via thermal degradation of methanol. This is the reason behind methane formation.

The weight hour space velocity (WHSV) is the weight inlet of methanol as fraction of the weight of catalyst. The weight inlet flow of methanol is determined with the Antoine Equation and the ideal gas law (Winkelman, 2020). At equilibrium, the Gibbs energy of both the liquid and vapour phase are the same. If the liquid and vapour are in equilibrium, the pressure is equal to the vapour pressure. With the Gibbs Energy Equations, a relation between the vapour pressure and the temperature could be obtained, the Antoine Equation. For many compounds, the constants in the Antoine Equation are tabulated. The Antoine equation is only valid for a certain temperature range. The following form of the Antoine Equation is used (with corresponding values for methanol (Dortmund Data Bank (DDB), n.d.)):

$$P = 10^{A-\frac{B}{T+C}}$$

$$A = 8.08097$$
$$B = 1528.27$$
$$C = 239.7$$
$$15°C < T < 100°C$$

With the obtained partial pressure, the Inlet weight flow of methanol could be determined. To do this the ideal gas law is used. The total derivation for determining the inlet weight flow of methanol with the ideal gas law is shown in appendix A.

To change the WHSV two parameters could be changed. These parameters are the gas flow of the carrier gas nitrogen or the amount of catalyst. However, there are restrictions when changing the temperature of the methanol saturator and the N_2-flow. If the N_2-flow is too high, no methanol conversion is obtained. The reason for this is a too low residence time. The methanol is transported too quickly through the reactor. A low flow rate correspond to a high residence time. This high residence time leads to high conversion. The problem with a low flow rate is that the total reactant flow per collection time (every two hours) is too low. This makes it impossible to collect liquid products. The temperature of the methanol saturator is not a possibility to change the WHSV, because it changes both the WHSV and the partial pressure. In this way the independent effect of the WHSV cannot be determined.

Decreasing of the N_2 flow is not an option, because it leads to a too low reactant flow per collection time. Also increasing the N_2-flow is not possible, because from earlier experiment it is found out that already at a WHSV of 9 the methanol conversion is low. This is the reason why in this project the amount of catalyst is used to change the WHSV. To investigate to influence of the weight hour space velocity, three different values for the WHSV are used. These values are 5, 7 and 9 hr^{-1}.The amount of catalyst that is used in the Packed Bed Reactor (PBR) is 0.35, 0.25, 0.20 g, respectively. The values for the weight hour space velocities are obtained with an Excel sheet (Figure 1).

	A	B	C	D	E	F	G	H	I	J	K	L	M	N	O	P	Q	R
1	Antoine equation								Pmethanol	0,35387	Bar				WHSV			
2									Ptotal	1	Bar				Mass catalyst	0,2	g	
3	P=10^(A-B/(C+T)								Fnitrogen	41	ml/min				ZSM	$Na_nAl_nSi_{96-n}O_{192}\cdot 16H_2O$ (0<n<27)		
4									Ftotal= Fmethanol + Fnitrogen						n=4	Al/Si=23		
5	Methanol								Fmethanol = x									
6	A	8,08097													Molar mass MeOH	32,04	g/mol	
7	B	1582,27							x/(x+41)= Pmethanol/Ptotal									
8	C	239,7							x=(Pmethanol/Ptotal)*(x+Fnitrogen)						PV=nRT	n=PV/RT		
9	T	40							x=((Pmethanol/Ptotal)*Fnitrogen)/(1-(Pmethanol/Ptotal))						n	0,00091	mol/min	
10									Fmethanol	22,455	mL/min				Fmass,MeOH	0,02904	g/min	
11									Ftotal	63,455	mL/min				Fmass,MeOH	1,74233	g/hr	
12	P	265,427	mmHG															
13		0,35387	Bar															
14															WHSV=Fmass,MeOH/Weight catalyst			
15															WHSV	8,71167	hr^-1	

Figure 1: Screenshot Excel sheet WHSV calculations

The goal of this project is to investigate strategies to supress coking, which is a drawback of the MTA-process. If from research solutions could be found to supress coke formation, this process could be successfully commercialized, like MTO and MTP. In this project the influence of the weight hour space velocity (WHSV) and the modification of magnesium of the catalyst are the used strategies to see what the effect on coking is. It is expected that decreasing the WHSV, which means increasing the amount of catalyst, decreases coke formation. Another expectation is that magnesium will change the acidity of the HZSM-5 catalyst, like other metal ions (Li et al., 2021).

Experimental

Chemicals

The used HZSM-5 zeolite catalyst (SiO_2/Al_2O_3 molar ratio of 23) was obtained in the ammonia form from Zeolyst International (product No. CB-V2314) (He et al., 2021). Methanol (≥99,9%, CAS no. 67-56-1) was supplied by Sigma Aldrich. Nitrogen used as carrier gas was obtained by Linde.

Catalyst preparation

The ZSM-5 catalyst is modified with Mg metal ions. This is done with a technique called incipient wetness impregnation. Incipient wetness impregnation is the most widely used method for the preparation of heterogeneous catalysts (Sietsma et al., 2006). During incipient wetness impregnation the catalyst is impregnated with a solution that contains the precursor, in this case a solution of $MgNO_3{\cdot}6H_2O$. After impregnation, the product is dried and then further treated. Further treatment in this case means calcination. After calcination, the impregnated catalyst is sieved to a sieve fraction of 300-500 µm.

The following procedure is followed for the incipient wetness impregnation: A round bottom flask was taken in combination with a stirring egg. 500 mg of catalyst was weighted and added to the round bottom flask. The amount of $MgNO_3{\cdot}6H_2O$ is determined depending on the weight percentage needed. The amount determined was multiplied by a factor 10 and weighted. The $MgNO_3{\cdot}6H_2O$ was dissolved in 1.75 mL water. 0.175 mL of this solution was taken and added dropwise to the catalyst while stirring. The amount of catalyst after impregnation was weighted and then transported to a small flask. The flask was covered with aluminium foil in which small pores were made. The flask was put in an oven at 120°C and was heated overnight.

Catalyst characterization

The acidity and structure of the HZSM-5 catalyst and the magnesium impregnated catalyst were both analyses. The analysis of the structure is done both wit X-ray diffraction (XRD) and with N_2-physisorption. For XRD a D8 Advance Powder Diffractometer with Cu Kα radiation was used (He et al., 2021). It was operated at 40 kV and 40mA. The D8 Advance Powder Diffractometer is combined with a LYNXEYE detector, which has a 2θ scan range of 5-50°. For the XRD analysis samples of 0.200 g were used. The N_2-physisorption is performed with an ASAP 2420 Surface Are and Porosity Analyzer to obtain Nitrogen Isotherms at 77.3 K (He et al., 2021). The surface was determined with the Brunauer-Emmett-Teller (BET) method. This is done by using the adsorption isotherms in the P/P_0 range of 0.05-0.25.

The total acidity of the used catalysts is determined with NH_3-TPD. The analysis is performed with an Autochem II 2920 using ammonia (He et al., 2021). The catalyst samples were placed in the analyser at 550°C under helium flow (50 mL, 1h) and consequently cooled down to 100°C. Then the catalyst was saturated with ammonia in helium (1.0 vol%, 50 mL min^{-1}) for one hour. The samples were purged with helium to remove weakly absorbed ammonia.

In the last step desorption of ammonia takes places in which the samples were heated again to a temperature of 550°C (temperature ramp of 10°C min^{-1}).

The spent catalyst is analysed with thermogravimetric analysis. The thermogravimetric data was obtained with a TGA 4000 Analyzer (He et al., 2021). The samples were heated from 50 to 700°C (temperature ramp of 10°C min^{-1}) under an air flow of 50 mL min^{-1}. The amounts of carbon and hydrogen on the spent catalyst were determined with an elemental analyser (EuroEA3000, Eurovector, Italy).

Catalyst activity test

Setup

The used setup could be divided into three different parts: the methanol saturator, a packed bed reactor and the condenser. In appendix B the piping and instrumentation diagram is shown. The first part of the setup is the nitrogen storage tank. This tank is used to storage and deliver the carrier gas, which is in this experiment nitrogen. The amount of nitrogen that flows into the system is controlled with a flow indicator controller. After the flow indicator controller, the gas line is split into two different tracks, a bypass track and the tracks that leads to the methanol saturator. The bypass track is used when no reaction should take place. In the methanol saturator the nitrogen carrier gas transport the methanol via a heating line to the reactor. The heating line is used to ensure a homogeneous mixture without condensation. In this part of the setup the first check valve is placed, to ensure that the gas stream only flows in the direction of the reactor. In the reactor the HZSM-5 catalyst is placed while operating at a temperature of 450°C. After the reactor, a control valve is placed and after that a second check valve is placed. The gas stream is then transported to the last part of the setup, which is the condenser. At the bottom, the liquid product is separated from the vapour product. The vapour product stream is connected to a three-way valve, in which the other outlet is the vent.

Methanol to aromatics Reaction

The Methanol to aromatics reaction was carried out with the setup described above. Before the reaction, it was checked if the bypass mode was on. It was also checked if the vent vale worked well. Then it was checked if the N_2-bottle was open and that the right pressure (2 bar) was set. The N_2-flow was set to zero and then the reactor was lowered to remove the U-tube. The used catalyst was collected, and the tube was cleaned with air and acetone. 0.200 mg of ZSM-5 catalyst (300-500 µm) was weighted and added to the tube. Grease was added to the end of the tube to ensure air-tightness and the tube were placed back in the reactor with springs. It was checked if the methanol saturator was on at a temperature of 40°C. A temperature of 40°C is used to obtain a partial pressure of methanol of 354 mbar. This results in a weight hour space velocity of methanol of 9 h^{-1}.

Besides the saturator, also the heater, controllers and coolers were checked if these were on and set to the right temperature. A leakage check was performed and after this the 2-way ball valve was opened again. The N_2-flow was set to 41 mL/min and the reactor temperature was set to 150°C. Consequently, the temperature of the reactor was increased to 450°C with an increment of 50°C. After the valves were changed to normal mode, the pressure drops shortly because of empty spaces that were filled. After this the reaction was started and every two hours a gas and liquid sample were taken. A gas sample was taken by turning the vent valve towards the reaction of the gas sample outlet. Before turning the valve, a syringe was put on the outlet of the valve. When the sample was taken the valve was turned back to the vent side. A liquid sample was taken with the liquid product valve. A liquid sample was taken by positioning the vent valve perpendicular to the vent outlet, to stimulate liquid to come out.

When the reaction was done addition of methanol was stopped. This was done by setting the valves to “bypass” mode. Then the heater of the methanol saturator and the heating line were turned off. The setup was flushed with N_2 for 15 minutes, and then the temperature of the reactor was set to 20°C. The N_2-flow was set to ~8 ml/min and all the other electric devices were turned off.

Results

Characterization catalyst

NH3-TPD

The acidity of the HZSM-5 catalyst and the 3 wt% Mg impregnated catalyst is determined with NH_3-TPD. In figure 2 the NH_3-TPD data is shown graphically. The HZSM-5 catalyst shows two peaks at 225°C and 400°C. This is in line with the values found in literature for the HZSM-5 catalyst (He et al., 2021; Niu et al., 2020). In literature it is stated that the peak around 200°C corresponds to weak acid sites, while the peak around 400°C corresponds to strong acid sites. After magnesium impregnation the acidity of the catalyst decreases extensively. There is no peak around 400°C, which indicates that the strong acid strength of the catalyst is reduced. The peak corresponding to the weak acid sites is shifted towards lower temperature, which means that also the weak acid strength is reduced (Niu et al., 2020). So, the NH_3-TPD data shows that magnesium impregnation decreases the acid strength of the HZSM-5 catalyst.

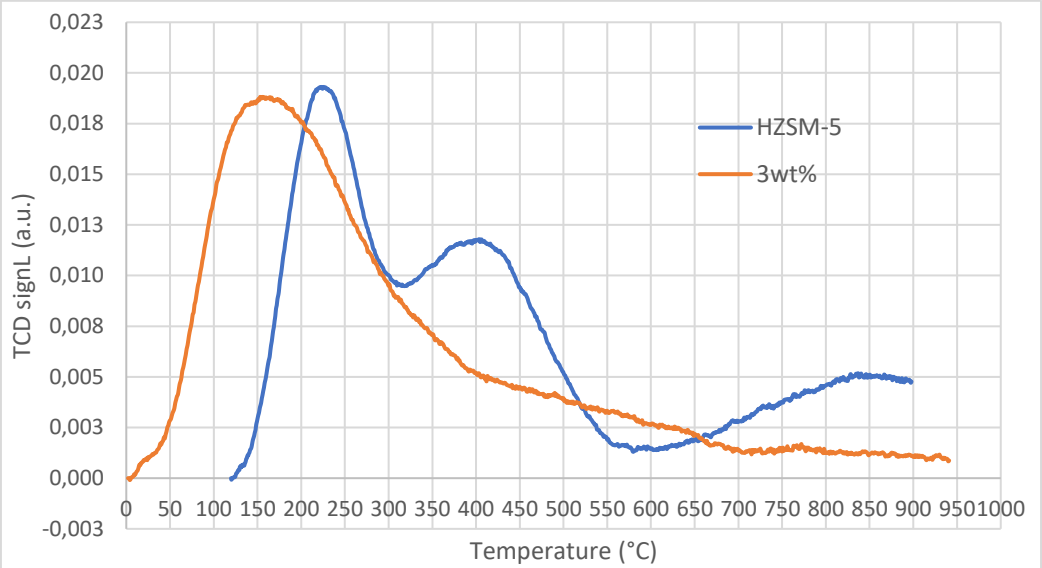

Figure 2: NH_3-TPD diagram of HZSM-5 catalyst and 3 wt% magnesium impregnated catalyst

Nitrogen physisorption

The structure of the magnesium impregnated HZSM-5 catalyst is analysed with nitrogen physisorption. The total surface are (S_{BET}) is determined with the Brunauer-Emmett-Teller theory. The external area (S_{ext}) and the micropore area (S_{micro}) are determined with the t-plot method, and the same holds for the microvolume (V_{micro}). The pore width is calculated both with the BET-method and the BJH-method. The pore volume and the pore width, which are determined with the BET-method, were only obtained for the HZSM-5 catalyst and the 1wt% magnesium catalyst. Due to measuring issues, it was not possible to obtain these data for the other catalysts.

Table 1: Nitrogen physisorption data of HZSM-5 catalyst and different wt% magnesium impregnated catalysts

Sample	S_{BET} (m^2/g)	S_{EXT} (m^2/g)	S_{micro} (m^2/g)	V_{pore} (cm^3/g)	V_{micro} (cm^3/g)	Pore width Desorption BJH (nm)	Pore width BET (nm)
HZSM-5	275	71	203	0,1597	0,099	5,3319	2,32454
1%Mg/HZSM5	318	67	251	0,1887	0,1252	4,1422	2,37432
3%Mg/HZSM5	292	58	234		0,1202	4,7556	
5%Mg/HZSM5	294	51	243		0,1195	5,0557	
7%Mg/HZSM5	288	51	237		0,1164	4,828	

The data in table 1 shows that the total surface area remains constant after magnesium impregnation. The total surface area of the 1 wt% sample is slightly higher in comparison to the other values, but it could still be assumed that the total surface area does not change. This is not the case for the external surface area. The external area decreases from 71 m^2/g to 51 m^2/g, which is a decrease of 28%. The reason for this is dispersion of Mg species over the external area**.** This decrease in external area due to metal ions impregnated in the catalyst is in line with literature (Niu et al., 2020; Zhu et al., 2019) The micropore area and micropore volume are not changing after magnesium impregnation. The values of the unimpregnated catalyst are slightly lower. The reason for this is that the unimpregnated catalyst is not analysed at the same time as the other samples. The last measured characteristic is the pore width, which keeps constant too. The constant values of the micropore area, micropore volume and the pore width indicate that no magnesium blockage occurs in the micropores and that the pore structure does not change after impregnation with magnesium.

Isotherm plots

In figure 3 the isotherm plot of the unmodified zeolite catalyst is shown. The plot shows type I isotherms at low relative pressures, while at higher relative pressures type IV isotherms are visible by increasing nitrogen uptake (He et al., 2021). The type I isotherm plot indicates a microporous material, while the type IV isotherm indicates capillary condensation in larger mesopores (non-microporous contributions). This leads to a hysteresis loop which closes at a relative pressure of around 0.4 (Sing, 1982) . This small hysteresis loop shows that slit-shaped inter-crystalline voids (interparticle spaces) are present in the structure of the HZSM-5 catalyst (He et al., 2021).

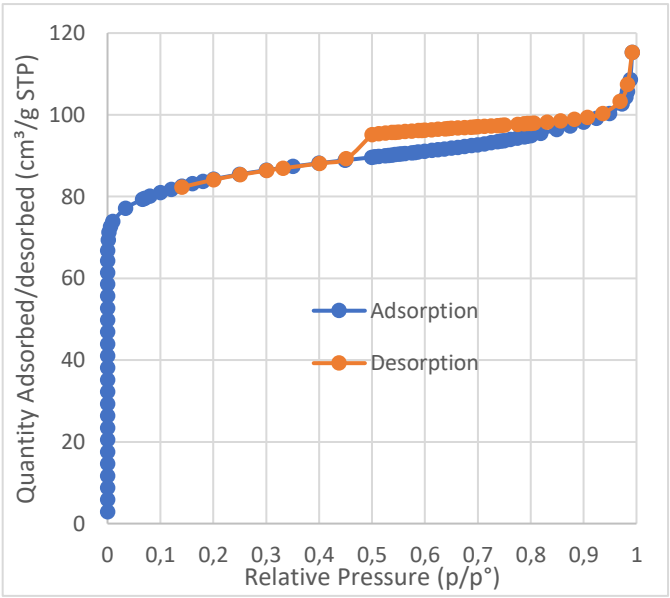

Figure 3: Isotherm plot of HZSM-5 catalyst

In figure 4 the isotherm plots of the impregnated catalysts are shown. The four different samples with different weight percentage of magnesium show all the same trend. In comparison with the unimpregnated catalyst, the type I isotherm is not visible in the isotherm plot. The reason for this is that the measurements of the impregnated catalysts the relative pressure range is between 0.05 and 1. Because the measurements were not started at a relative pressure of 0, the type 1 isotherm is not visible.

The type 4 isotherm is visible in all the impregnated catalysts, which indicates that the slit-shaped inter-crystalline voids are also present in the impregnated catalysts (He et al., 2021). The isotherm plots shows that the crystalline structure is not changed after magnesium impregnation.

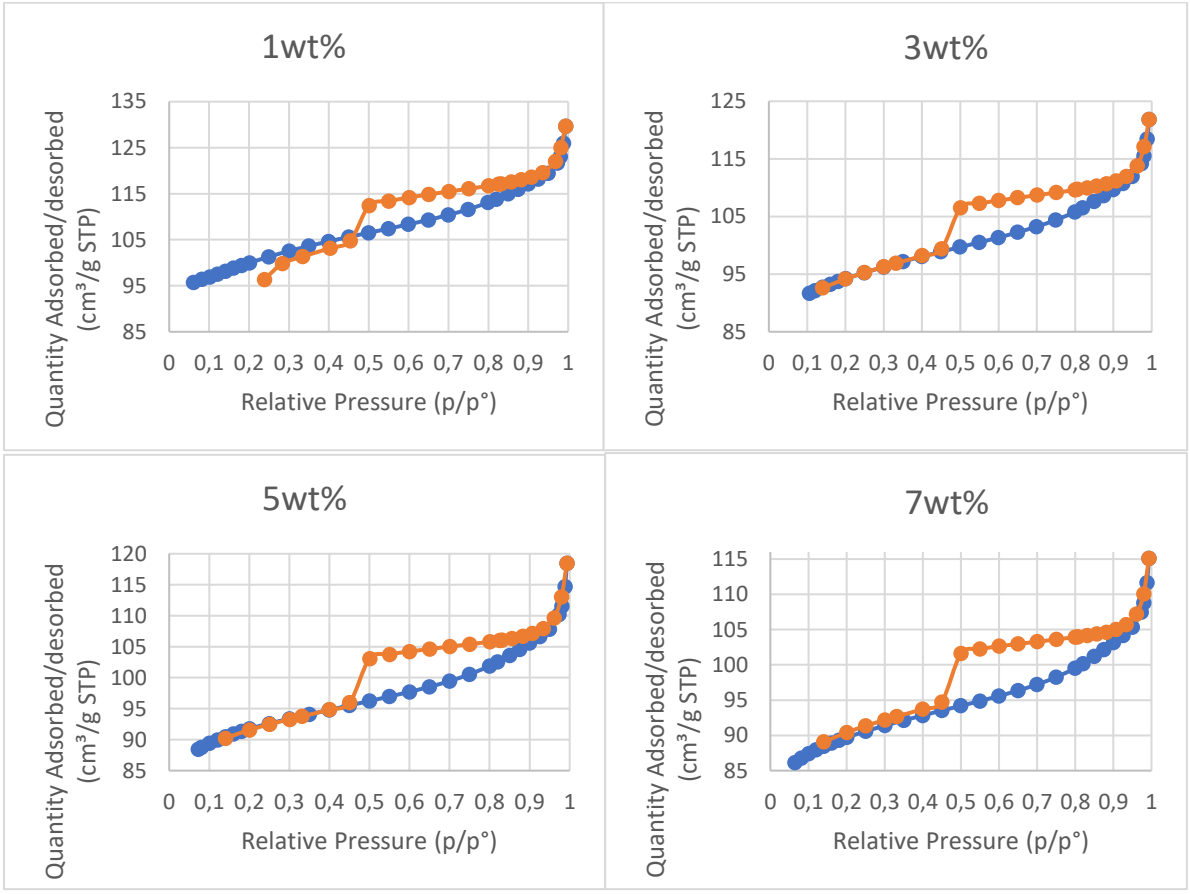

Figure 4: Isotherm plots of different wt% magnesium impregnated catalysts

Pore size distribution plot

In figure 5 the BJH desorption pore size distribution plot is shown. These plots are used to calculate the meso-pore size distribution (He et al., 2021). Mesopores are pores that have a pore width between 2-50 nm (Rouquerol, 1994). From literature it is found that the peak around 4 nm in the pore size distribution is an artifact (He et al., 2021). The 1 wt% sample shows a peak around 3 nm. This peak indicates that the 1 wt% sample has small mesopores. From the other graphs it could be concluded that no large mesopores are formed due to magnesium impregnation.

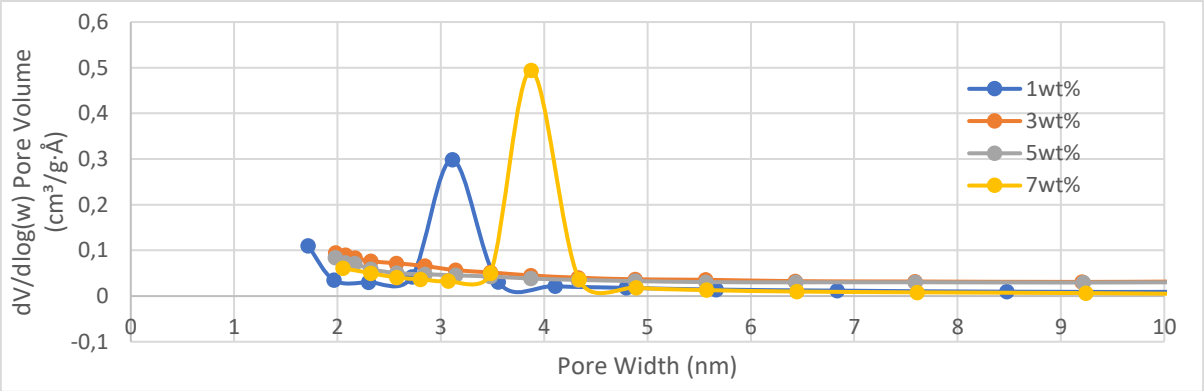

Figure 5: Pore size distribution plot of different wt% magnesium impregnated catalysts

X-Ray diffraction (XRD)

The morphology of the HZSM-5 catalyst and the impregnated catalysts is analysed with X-ray diffraction (XRD). The obtained XRD-diagrams are shown in figure 6 The comparison of the impregnated catalysts show similar peaks, which indicates that the different amounts of magnesium impregnated into the zeolite catalyst did not influence the structure.

The peaks of the impregnated catalysts (B-E) show also similar peaks to the unimpregnated catalyst (A). So, in general magnesium impregnation, no matter the amount of magnesium, does not influence the structure, which is in line with the nitrogen physisorption data.

In figure 7 the theoretical plot of a HZSM-5 catalyst is shown (Structure Commission of the International Zeolite Association (IZA-SC), 2017). This graph corresponds to a highly crystalline MFI-type zeolite. Comparison of this graph with the graphs of the impregnated catalyst, shows that no new diffraction peaks are observed. This indicates that impregnation of magnesium do not destroy the MFI structure of the HZSM-5 catalyst and that the magnesium particles are highly dispersed in the zeolite catalyst. This is in line with observations in literature (Niu et al., 2020).

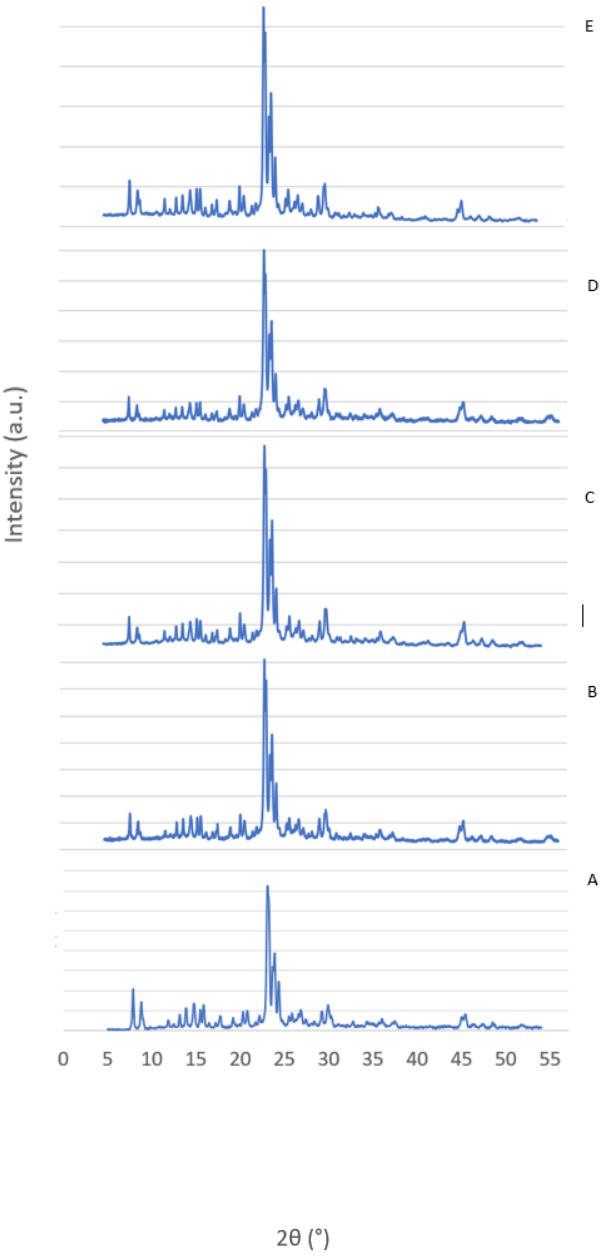

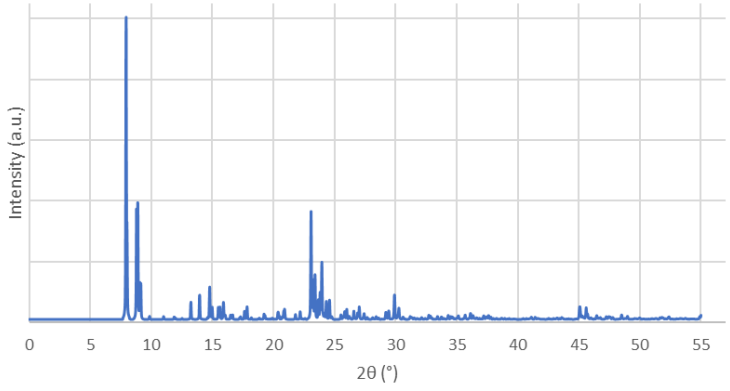

Figure 6: XRD patterns of a) HZSM-5, b) 1wt%, c) 3 wt%, d) 5wt%, e) 7wt%

Figure 7: Theoretical XRD-pattern of HZSM-5 catalyst

Catalytic performance WHSV

Gas chromatography

Samples of the obtained gas products were collected every two hours, which were then analysed with gas chromatography. The concentration of the compounds was determined with a reference sample. The concentrations (as percentage) of the components in the reference sample are known, see table 2. Combining these values with the areas of the components in the reference sample, the concentrations of the product samples could be determined. The selectivity of the components is defined as the concentration of the component as a fraction of the total concentration. The determined selectivity's of the components in the product samples are shown in table 3.

Table 2: Concentrations in reference sample

Concentrations in reference %	
CO2	17,9
Ethylene	0,509
Ethane	1,5
Propylene	0,512
Propane	1,49
H2	54,399
CH4	20,7
CO	2,99

Table 3: Selectivity's of gas products at different WHSV values a) WHSV=9, b) WHSV=7, c) WHSV=5

	Experiment 1			Experiment 2			Experiment 3		
Compound	2h (a)	4h (a)	6h (a)	2h (b)	4h (b)	6h (b)	2h (c)	4h (c)	6h (c)
Methane	0,464	0,541	0,589	0,425	0,472	0,473	0,415	0,448	0,509
Ethylene	0,356	0,308	0,268	0,343	0,315	0,304	0,347	0,321	0,295
Ethane	0,019	0,014	0,013	0,024	0,016	0,012	0,028	0,022	0,017
Propylene	0,154	0,132	0,127	0,138	0,144	0,164	0,136	0,151	0,136
Propane	0,007	0,005	0,003	0,070	0,053	0,047	0,073	0,058	0,044

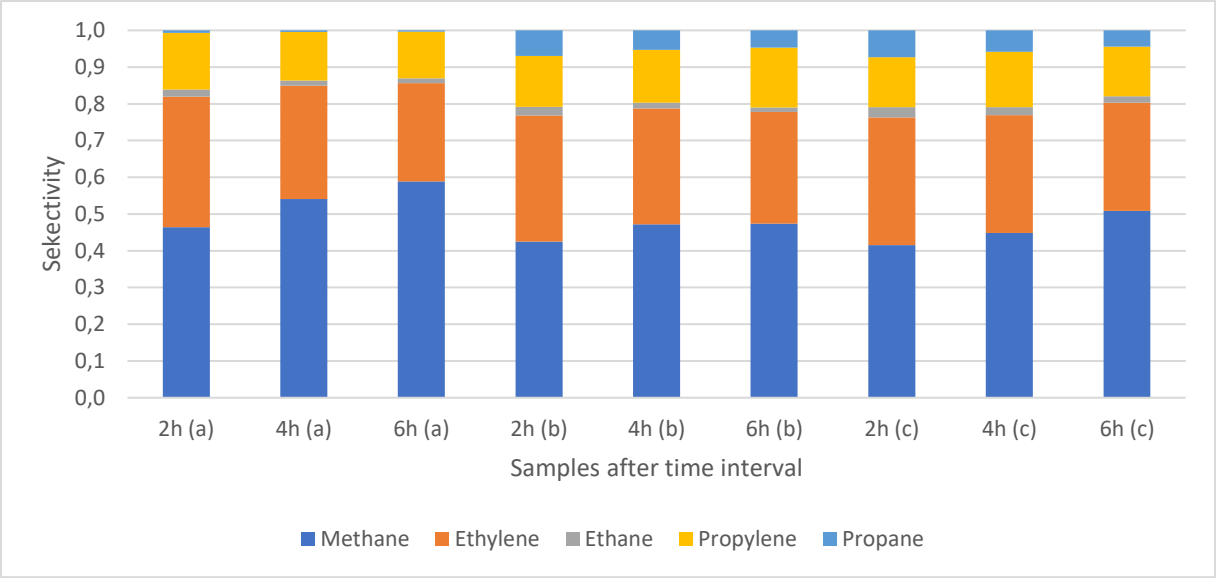

Figure 8: Block diagram of gas products at different WHSV values a) WHSV=9, b) WHSV=7, c) WHSV=5

The data in table 3 is shown graphically in the block diagrams in figure 8. The block diagram shows that the results of all the sampels are quite consistent. The methane selectivity is the highest (40-50%) and increases over time. Methane formation is caused by thermal degradation of methanol (Shoinkhorova et al., 2021). The increasing selectivity over time indicates that the thermal degradation of methanol increases over time. In literature it is stated that methane formation is favorable at higher WHSV for a MTH reaction with a nano-HZSM-5 catalyst (Zhao et al., 2014). The diagram shows that at higher WHSV the methane selectivity is higher. So the obtained data is in line with literature.

Because of the fact that the methane selectivity increases, the selectivity's of the other components decreases over time. The diagram shows that the selectivity of the olefins is higher in comparison to their paraffins . This is not in line with the charachteristic of the H-ZSM5 catalyst. In literature it is found that this catalyst has a hight HTI-ratio (Zhu et al., 2019). This indicates that the selectivity of the paraffins is higher than the selectivity of the olefins. However, the results show a opposite trend. This could be explained by the mechanism of the dual cycle carbon loop. In the first step methanol is converted to olefins, while in the second step the olefins are converted to aromatics in two different ways in which hydrogen or paraffins are formed. A high selectivity of olefins indicates that the conversion of the olefins to aromatics is low. A second reason could be that the dehydrogenation reaction is favoured over the hydrogen transfer reaction. However, this is not in line with literature, which says that the hydrogen transfer reaction is favoured for the unmodified catalyts. So, low conversion of the olefins is the most plausible reason for the high olefin selectivity. The selectivity of ethylene is almost twice as large as the selectivtiy of propylene. This indicates that ethylene formation is favoured over propylene formation.

GC-FID liquid products

Besides the gas samples, also samples of the liquid products were taken every two hours and consequently analyzed with GC-FID. With the obtained areas the selectivity is determined. The

Table 4: Selectivity's of all liquid products divided into different groups at different WHSV values a) WHSV=9, b) WHSV=7, c) WHSV=5

selectivity is defined as the area of the component as fraction of the total area (with exclusion of the solvent area). In table 4 the selectivities of the samples are shown.

	Experiment 1			Experiment 2			Experiment 3		
	2h (a)	4h (a)	6h (a)	2h (b)	4h (b)	6h (b)	2h (c)	4h (c)	6h (c)
BTX	0,077	0,63	0,254	0,767	0,447	0,424	0,226	0,291	0,64
Benzene derivatives	0,098	0,204	0,717	0,138	0,261	0,273	0,282	0,342	0,288
Methylindene	0,053	0,000	0,000	0,000	0,000	0,018	0,000	0,042	0,037
Naphtalene +derivatives	0,772	0,166	0,029	0,096	0,292	0,284	0,492	0,325	0,034

The raw data of the samples showes that many components are formed. All these components were divided into four groups: BTX (Benzene, toluene and xylene), benzene derivatives, methylindene and napthalene with inclusion of its derivatives. The obtained data of the selectivites is shown graphically in figure 9.

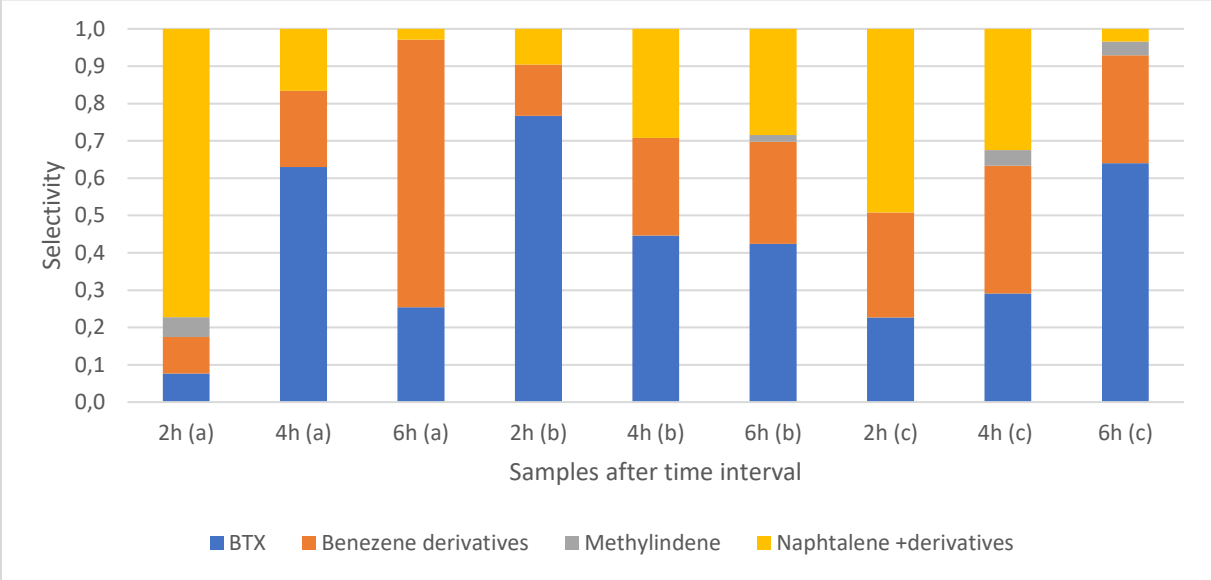

Figure 9: Selectivity's of all liquid products divided into different groups at different WHSV values a) WHSV=9, b) WHSV=7, c) WHSV=5

The graphs in figures 9 do not show a clear trend in selectivity's over time. The first sample in figure 9 shows a remarkably high selectivity of naphthalene and its derivatives. This value does not correspond with the values of the other samples. However, the selectivity of naphthalene + derivatives decreases over time. This is also the case for the measurements of the third experiment (c), but not for the measurements for the second experiment (b). A reason for this could be the high BTX selectivity after two hours. This value is large in comparison to the other BTX selectivity's. A reason for the decreasing naphthalene +derivatives selectivity could be that these components are involved in coke formation, which increases over time.

The selectivity of methylindene in figure 9 is in all the samples quite low (after 4h the selectivity is zero). The reason for this could be the same as for the naphthalene +derivatives group. All these molecules are large in comparison to the other components which makes it more likely to get stuck in the pores of the catalyst. In the measurements of experiment 3 (c) the methylindene selectivity is increasing slightly. However, a reason for this could be the decrease in selectivity of the naphthalene. Although this increase, the selectivity is still low.

The selectivity's of BTX and the benzene derivatives do not show a clear picture. This is especially the case for experiment 1 (a). However, the selectivity of the benzene derivatives is quite constant for experiment 2 (b) and experiment 3 (c). This is not the case for the BTX selectivity. However, this could be caused by the change in selectivity of the naphthalene group.

To get a clearer picture of the BTX and benzene derivatives fraction also the selectivity's of these groups are determined. In this case the selectivity is determined with the concentration of the BTX group and the benzene derivatives group as total concentration. The results are shown in table 5 and the corresponding graph is shown in figure 10.

Table 5: Selectivity's of BTX-components and benzene derivatives at different WHSV values a) WHSV=9, b) WHSV=7, c) WHSV=5

	Experiment 1			Experiment 2			Experiment 3		
Selectivity	2h (a)	4h (a)	6h (a)	2h (b)	4h (b)	6h (b)	2h (c)	4h (c)	6h (c)
Benzene	0,058	0,197	0,045	0,162	0,053	0,023	0,033	0,013	0,050
Toluene	0,096	0,288	0,080	0,383	0,202	0,123	0,080	0,101	0,218
Xylene	0,284	0,271	0,137	0,302	0,376	0,462	0,331	0,348	0,422
Benzene derivatives (C9)	0,410	0,110	0,612	0,106	0,302	0,325	0,453	0,444	0,272
Benzene derivatives (C10)	0,152	0,135	0,126	0,046	0,066	0,067	0,102	0,093	0,039

The graph in figure 10 shows that the selectivity of both benzene and C10 benzene derivatives is low in comparison to the other components. Both selectivity's are quite constant, this could indicate that the bigger C10 benzene derivatives could be involved in coke formation. The selectivity of toluene is slightly higher and in general quite constant. Only the samples 4h (a) and 2h (b) show a higher selectivity for toluene. The selectivity's of xylene and C9-benezene derivatives are the largest of all components. The values are fluctuating, but the combined selectivity of these two components is constant. The graph shows that in most of the samples the BTX selectivity is higher than the selectivity of the benzene derivatives.

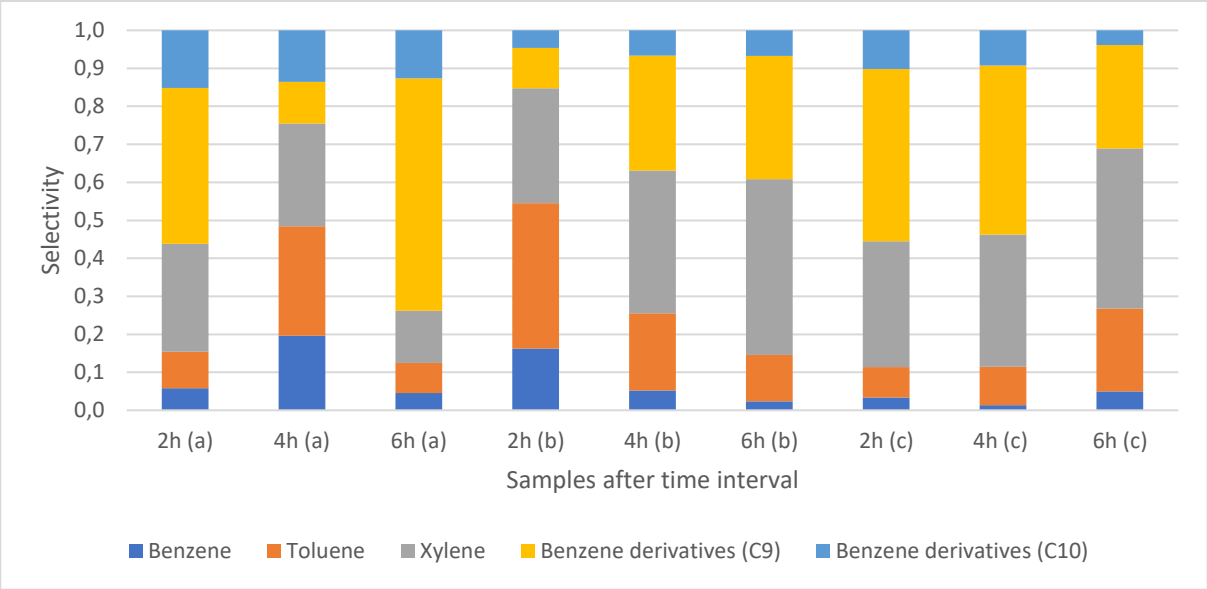

Figure 10: Selectivity's of BTX-components and benzene derivatives at different WHSV values a) WHSV=9, b) WHSV=7, c) WHSV=5

The last type of selectivity that is analysed is the selectivity of the BTX group. The selectivity's of the components are shown in table 6 and the corresponding graph is shown in figure 11.

Table 6: Selectivity's of BTX components at different WHSV values a) WHSV=9, b) WHSV=7, c) WHSV=5

	Experiment 1			Experiment 2			Experiment 3		
Selectivity	2h (a)	4h (a)	6h (a)	2h (b)	4h (b)	6h (b)	2h (c)	4h (c)	6h (c)
Benzene	0,133	0,260	0,174	0,191	0,083	0,038	0,075	0,029	0,072
Toluene	0,219	0,381	0,304	0,452	0,321	0,202	0,181	0,220	0,316
P-xylene	0,313	0,235	0,327	0,227	0,415	0,534	0,489	0,518	0,403
M-xylene	0,335	0,124	0,195	0,130	0,182	0,225	0,255	0,233	0,208

The graph shows that the WHSV does not influence the selectivity of the BTX-components. The selectivity's are overall quite constant. The selectivity of benzene is the lowest and decreases slightly at lower values for the WHSV. The selectivity of meta-xylene is also constant and is lower than the selectivity of para-xylene. This is indicating that para-xylene is favoured over meta-xylene. The selectivity's of para-xylene and toluene are fluctuating more than the other two components. The graph shows that the para-xylene selectivity is higher at lower values for the WHSV.

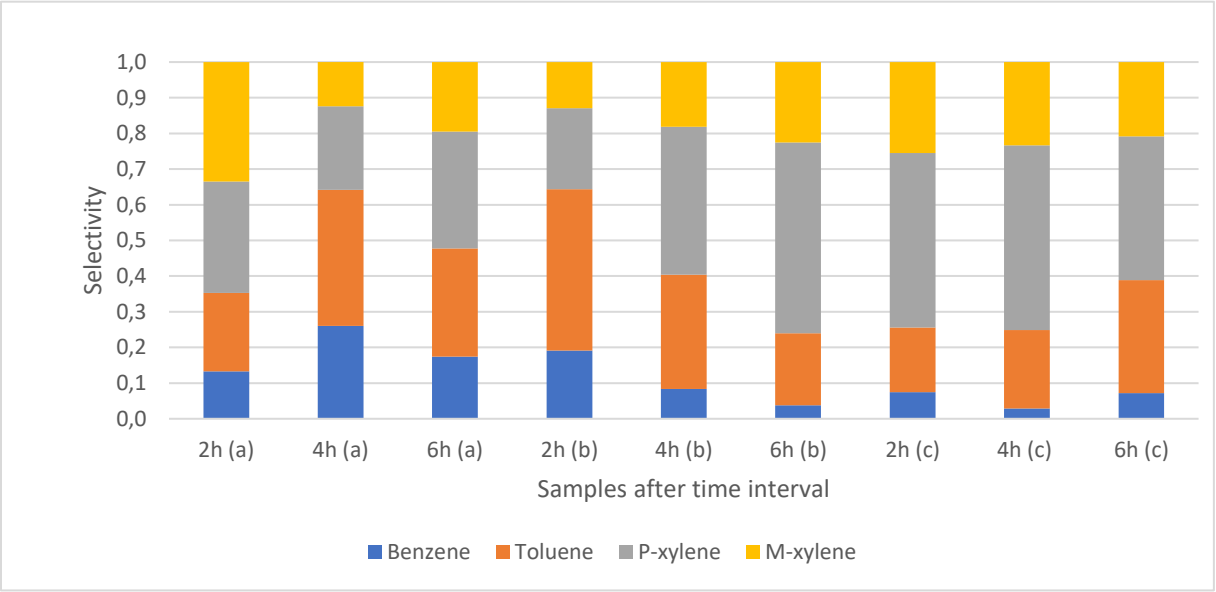

Figure 11: Selectivity's of BTX components at different WHSV values a) WHSV=9, b) WHSV=7, c) WHSV=5

Thermogravimetric analysis (TGA)

The spent catalyst is analysed with thermogravimetric analysis (TGA). In figure 12 the obtained TGA data is shown graphically. The graphs shows the weight loss of the catalyst over a certain temperature range. The plot shows that there are two ranges in which weight loss occurs. The first range is around 100°C, which corresponds to weight loss due to loss of water. This indicates that the HZSM-5 catalyst has an affinity for water. In the temperature range of 300-500°C the graph is horizonal, indicating that there is no weight loss. After 500°C there is a second temperature range in which weight loss occurs. This temperature range corresponds to decomposition of coke deposition (Niu et al., 2020).

During the experiment two layers are formed, a black layer and a grey layer. For the WHSV of 5 both layers are analysed separately, which means that the combined layer (like the blue and orange lines) should be between the yellow and grey line. The grey line correspond to the grey part of the spent catalyst. This line shows that the grey part undergoes less coking in comparison to the black part (yellow line). There is a difference of around 6 wt% weight losses, indicating the large difference in coke formation between the parts of the spent catalyst. After removal of the weight% of the catalyst is 97 wt%. Comparing this value with the end values after coke removal shows that the weight percentage of coke is around 11 wt% for WHSV of 9, and 8 wt% for a WHSV of 7. The average line corresponding to a WHSV of 5 should end around 91-92 wt%, which correspond to a coke weight percentage of around 6 wt%. The graph and these values show that deceasing the WHSV, and thus increasing the amount of catalyst, results in decreasing coke formation. The reason for this is the higher amount of catalyst at lower WHSV values. The TGA measures the average coke formation, and on average to coke formation is lower when the amount of catalyst is higher (larger part with lower coke formation). Decreasing coke formation when decreasing the WHSV is in line with literature. This is also the case in the MTG process (Wan et al., 2018).

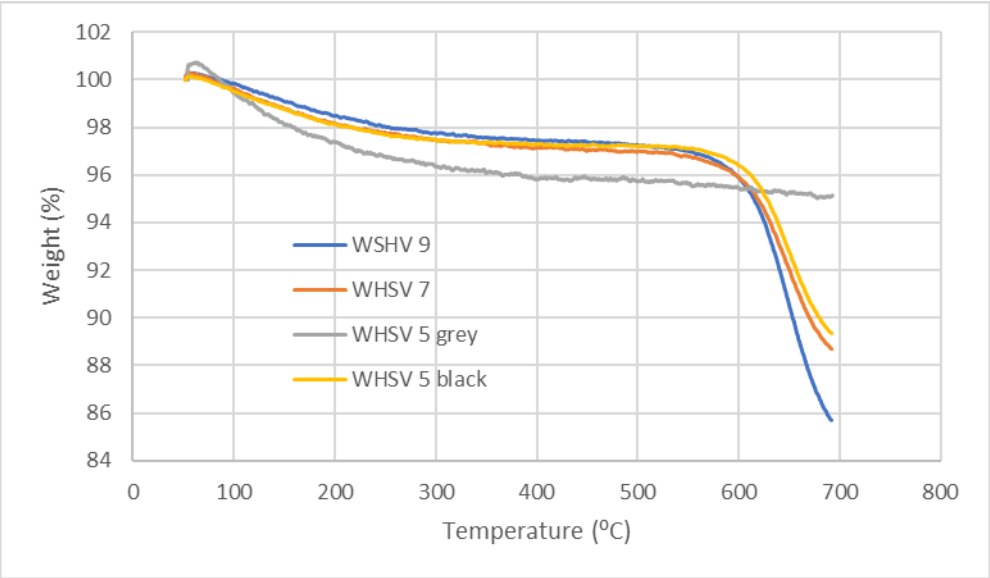

Figure 12: TGA diagram of spent catalysts at different WHSV values

Catalytic performance with magnesium impregnated catalyst

Gas chromatography

The obtained gas products are analysed with gas chromatography. With the obtained data the selectivity's of the formed gas products are obtained. These data are shown in table 7. The corresponding graphs are shown in figure 13. The graph shows that for the 3 wt% catalyst the methane selectivity is increasing after four hours, and then decreasing again. The 5 wt% shows the same trend as the samples of the WHSV experiments, in which the methane selectivity is increasing over time. The methane selectivity of both impregnated catalysts is higher than the selectivity's of the samples in the WHSV experiments. From literature it is found that methane formation is favourable at deactivated catalysts which are dominated by weak acid sites (Zhao et al., 2014). From the NH_3-TPD data it is obtained the after magnesium impregnation the total acidity of the catalyst decreases. This could be a reason for the higher methane selectivity. The graph shows that no paraffins are formed, which could be an indication for low aromatics formation via the dehydrogenation reaction. The selectivity's of the first two samples are quite similar for both catalysts. Only the samples after six hours differ a lot from each other.

Table 7: Selectivity's gas products of the two different catalysts with weight percentages of 3wt% and 5wt%

	3wt%			5wt%		
Compound	2h	4h	6h	2h	4h	6h
Methane	0,520	0,701	0,574	0,517	0,590	0,826
Ethylene	0,241	0,160	0,061	0,238	0,195	0,119
Ethane	0,009	0,000	0,000	0,000	0,000	0,000
Propylene	0,231	0,139	0,365	0,245	0,215	0,055
Propane	0,000	0,000	0,000	0,000	0,000	0,000

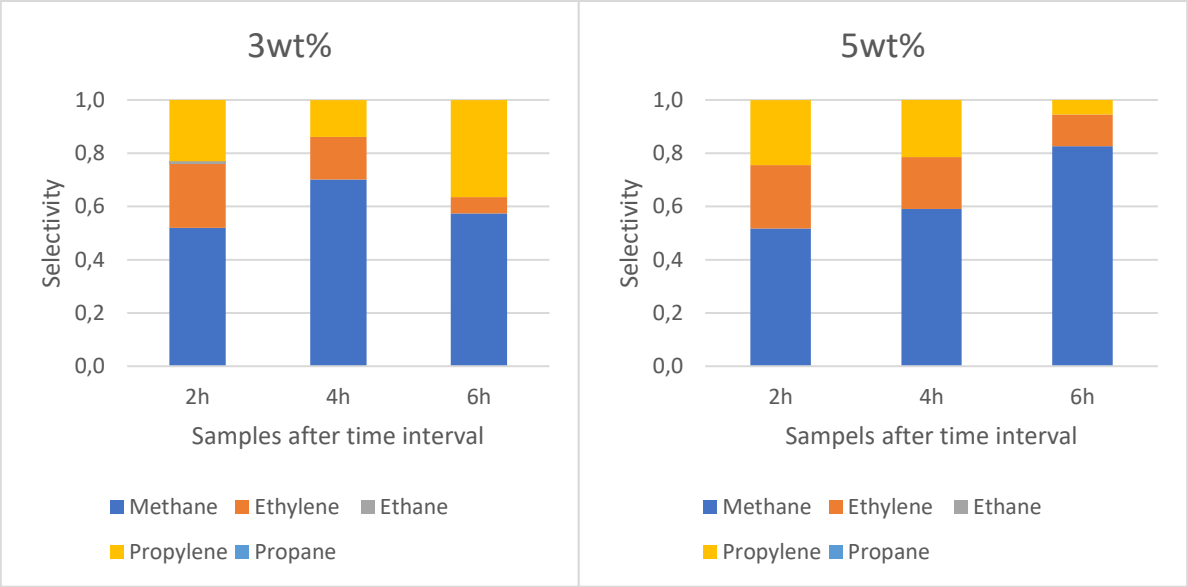

Figure 13: Selectivity's gas products of the two different catalysts with weight percentages of 3wt% and 5wt% magnesium

GC-FID liquid products

The liquid samples of the experiment with the impregnated catalyst is analysed in the same way as the liquid samples of the experiments with changing WHSV. Due to measuring issues, it was not possible to obtain data for all the samples. Nevertheless, the data of the samples that could be measured are shown in table 8 and figure 14. From figure 14 no general trend could be determined. In comparison to the values for the WHSV experiments, the BTX selectivity is much lower. A reason for this could be de decreased total acidity of the catalyst after magnesium impregnation, as shown in the NH_3-TPD data. In literature it is stated that strong acid sites are crucial for high methanol conversion and high yield of aromatics (Zhang et al., 2015).

Table 8: Selectivity's of all liquid products divided into different groups corresponding to the two catalysts with different weight percentages of 3 wt% and 5 wt% magnesium

	3 wt%			5 wt%		
	2h	4h	6h	2h	4h	6h
BTX		0,236	0,031	0,211	0,044	
Benezene derivatives		0,466	0,300	0,299	0,956	
Methylindene		0,000	0,477	0,113	0,000	
Naphtalene +derivatives		0,298	0,191	0,377	0,000	

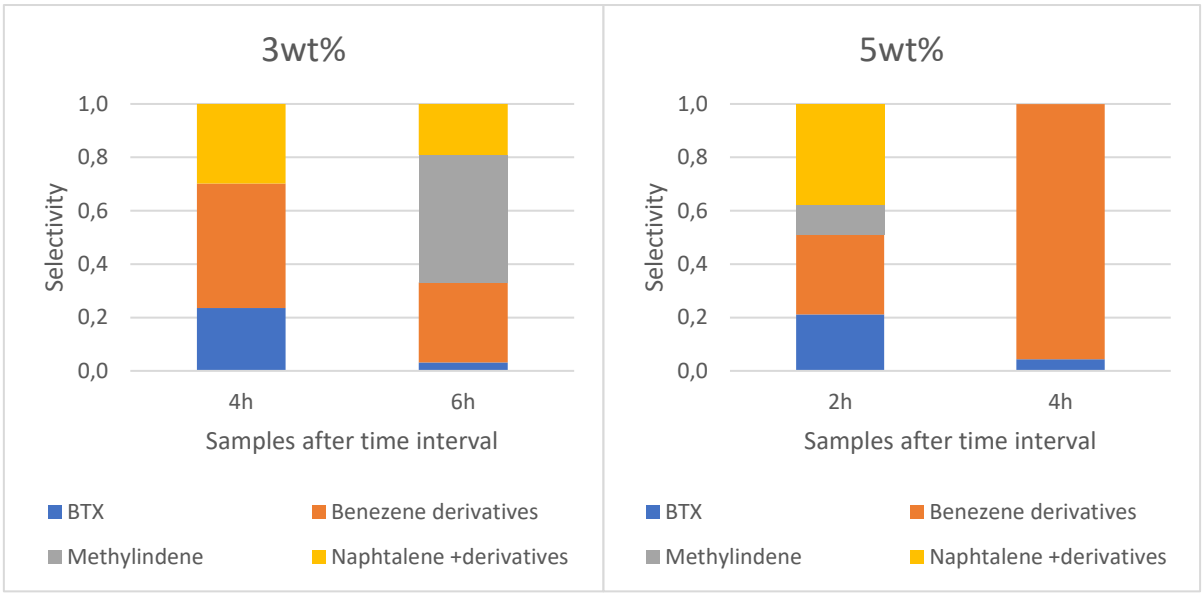

Figure 14: Selectivity's of all liquid products divided into different groups corresponding to the two catalysts with different weight percentages of 3 wt% and 5 wt% magnesium

This lower BTX selectivity is also visible in figure 15. In figure 15 the selectivity's of the BTX components and the benzene derivatives are shown. Due to the measuring issues no relevant results are obtained for the BTX and benzene derivatives selectivity. The last selectivity that is determined is the selectivity of the BTX-components. The data is shown in table 10 and in figure 16. The 3wt% samples show that the Para-xylene selectivity is the highest, which was also the case for the WHSV experiments. For the rest there are no relevant results because there are not enough data points.

Table 9: Selectivity's of BTX-components and benzene derivatives corresponding to the two catalysts with different weight percentages of 3 wt% and 5 wt% magnesium

	3 wt%			5 wt%		
Selectivity	2h	4h	6h	2h	4h	6h
Benzene		0,016	0,013	0,028	0,000	
Toluene		0,088	0,020	0,134	0,044	
Xylene		0,240	0,061	0,252	0,000	
Benzene derivatives (C9)		0,432	0,426	0,438	0,879	
Benzene derivatives (C10)		0,224	0,480	0,148	0,077	

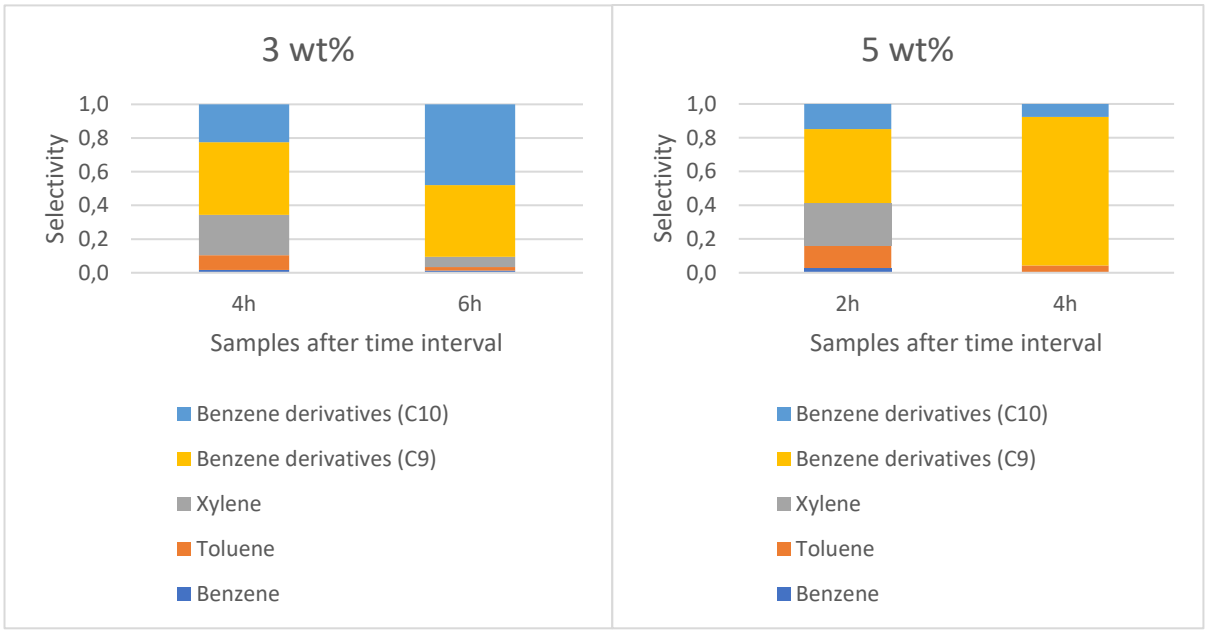

Figure 15: Selectivity's of BTX-components and benzene derivatives corresponding to the two catalysts with different weight percentages of 3 wt% and 5 wt% magnesium

Table 10: Selectivity's of BTX-components corresponding to the two catalysts with different weight percentages of 3 wt% and 5 wt% magnesium

	3 wt%			5 wt%		
Selectivity	2h	4h	6h	2h	4h	6h
Benzene		0,048	0,138	0,000	0,000	
Toluene		0,262	0,216	0,217	1,000	
P-xylene		0,524	0,398	0,757	0,000	
M-xylene		0,167	0,248	0,026	0,000	

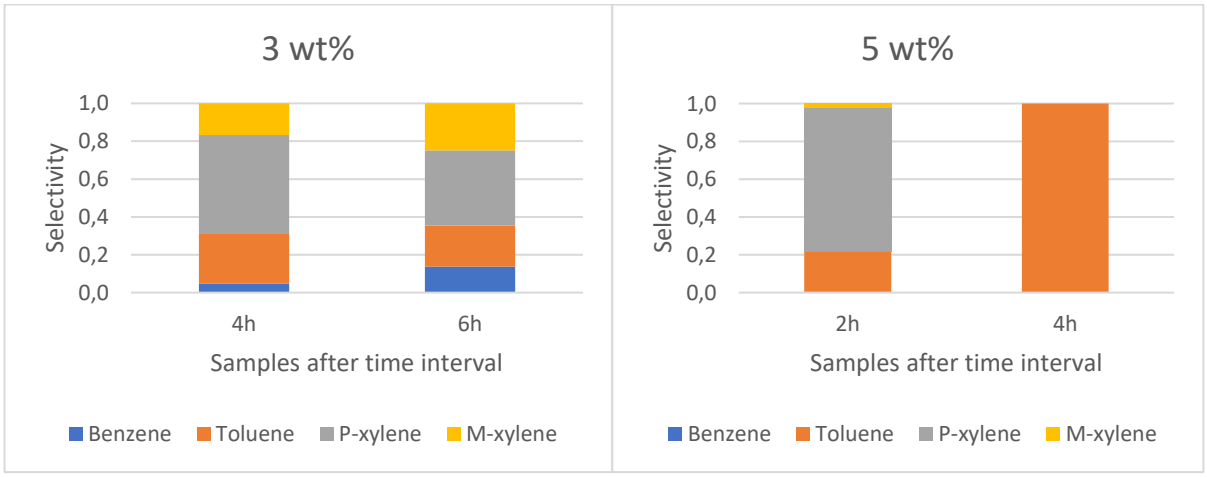

Figure 16: Selectivity's of BTX-components corresponding to the two catalysts with different weight percentages of 3 wt% and 5 wt% magnesium

Thermogravimetric analysis (TGA)

In figure 17 the thermogravimetric curves of the impregnated catalysts are shown. The graph shows that there are again two ranges in which weight loss occurs. The first range is again around a temperature of 100°C, caused by removal of water in the catalyst. The second range of weight loss is the same as for the unimpregnated catalysts. After weight loss due to water removal the weight% of the catalyst is decreased to 97 wt%. In the temperature range of 500-700°C a weight loss of 13% is visible for both catalysts, compared to the 97 wt%. From these TGA data it could be concluded that different weight percentages of magnesium in the HZSM-5 catalyst does not influence the coke formation. In comparison to the unimpregnated catalysts (weight loss equals 6-11%), the coke formation is even higher after impregnation with magnesium. This could indicate that impregnation of the catalyst has a bad impact on coke formation. The used catalyst was totally black, and no grey parts were visible. This is also an indication for higher coke formation. The higher coke formation is in line with the higher methane selectivity for the impregnated catalyst in comparison with the results of the WHSV experiments. As mentioned before, in literature it is stated that methane formation is favourable at deactivated catalysts which are dominated by weak acid sites (Zhao et al., 2014). A reason for the higher coke formation after magnesium impregnation could be the lower acidity of the catalyst. The lower acidity decreases the methanol conversion (Zhang et al., 2015) which could let to carbon build-up, and thus to higher coke formation.

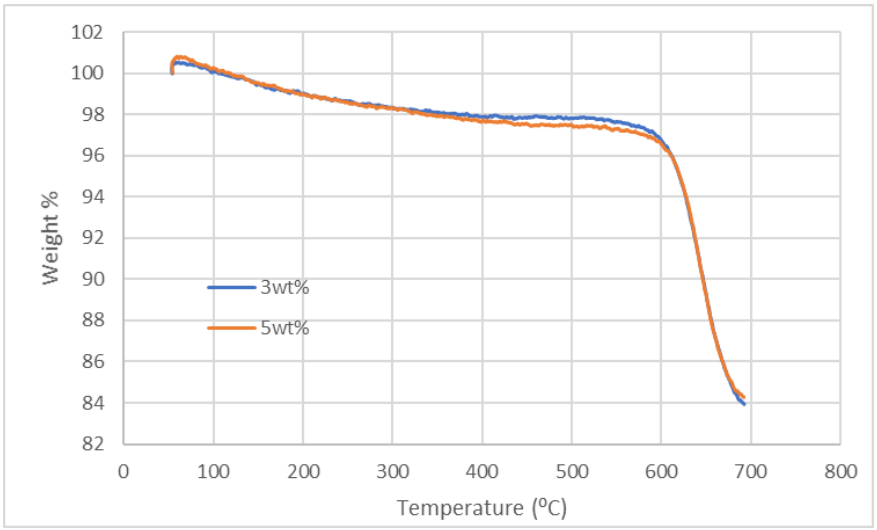

Figure 17: TGA diagram of the two catalysts with different weight percentages of 3 wt% and 5wt%

Discussion

The results of the gas and liquid products show that they could only be analysed with gas chromatography to determine the selectivity's of the formed products. However, the selectivity's of the products do not give a complete picture of the product formation. Besides the selectivity, the yield of the products is necessary to give conclusions and justifications. This could be solved by implementing internal standards in the GC-measurements. The methanol conversion is also important data that is missing in this experiment. Methanol conversion is especially important to determine the effect of changing the WHSV or the acidity of the catalyst. If the products samples do not show any methanol present, this indicates that full conversion is obtained. However, this does not say anything about the methanol conversion inside the catalyst (at the acid sites). From the results of the magnesium impregnation, it seems that the methanol conversion is lower, but there is no hard evidence for that. Another aspect that reduces the significance of this report is the number of data point. Three data point is not enough to determine data trends.

Also, in case of measuring issues, which was the case for the GC-FID measurements of the liquid samples, three data samples are not enough in case of measuring problems.

Future perspectives

Further research regarding the influence of the WHSV on the coke formation is recommended. As mentioned in the discussion, implementing the methanol conversion and product yield data points are giving a much better picture of the effect of the WHSV on the coke formation. Also, a wider range of WHSV values could be analysed, to see if the effect of WHSV does not influence the amount of coking after a certain range. In research magnesium is combined with other modifications, such as phosphorous and zinc (Zhu et al., 2019). Further research could be done to determine if magnesium could decrease the coke formation.

Conclusions

In the first part of this project the effect of WHSV on the coke formation is determined. The analysis of the gas products with gas chromatography shows that methane has the highest selectivity (40-50%). Methane is formed via thermal degradation of methanol. The methane selectivity increases when the WHSV increases, which is in line with literature. The selectivity of the olefins is much higher in comparison to the paraffins, which could indicate that the conversion of olefins to aromatics is low. The selectivity's of the liquid products does not show a clear trend. However, if the naphthalene and methylidene products are neglected, the selectivity of benzene and C-10 benzene derivatives is low. A reason for the low C-10 derivatives selectivity's could be that these components are involved in coke formation. The BTX-selectivity shows that p-xylene is favoured over m-xylene. At lower WHSV the p-xylene selectivity increases. The TGA data shows that coke formation decreases at lower WHSV. This is in line with literature. The reason for this is that at lower WHSV more catalyst is used, which decreases the average coke formation, which is measured during TGA. In literature it is found that methane selectivity is favoured when the catalyst is deactivated. So, a higher methane selectivity at higher WHSV is in line with the TGA data.

The catalyst is characterized with XRD, TPD-NH_3 and nitrogen physisorption. The XRD and nitrogen physisorption data shows that the crystalline MFI structure of the catalyst is not changed after magnesium impregnation. The NH_3-TPD data shows that the total acidity of the HZSM-5 catalyst has decreased after magnesium impregnation.

The analysis of the formed gas products after the measurements with the magnesium impregnated catalyst shows that the methane selectivity is higher in comparison with the values of the WHSV experiments. The reason for this could be the lower acidity of the impregnated catalyst, which decreases the methanol conversion. No paraffins are formed, which could be an indication for low olefin conversion to aromatics. Due to measuring issues during the liquid product samples no relevant data was obtained. The TGA data shows that magnesium impregnation increases coke formation. This is probably caused by the lower acidity, which decreases the methanol conversion. This led to carbon build up, and consequently to coke formation.

Further research could be done in determining the methanol conversion and determining the yield of the product via internal standards. Also increasing the data point and the number of experiments is recommended to get better and more reliable results.

Acknowledgement

During this project I received a lot of assistance and help. Firstly, I would like to thank my supervisor, dr. ir. Jingxiu Xie. Your assistance and knowledge inside and outside the lab helped me in discovering and learning the research area of heterogeneous catalysis for gas conversion. I would also thank my second supervisor Prof. dr. Jun Yue. Doing this project was impossible without the help of all the research assistants doing the analysis. I want to thank Paresh Butolia (NH_3-TPD, liquid GC), Felipe Orozco (TGA), Jessi Osorio (GC, XRD), Qingqing Yuan (Nitrogen physisorption) for doing the analysis, especially in these times of Corona which bring a lot of restrictions. Besides the analysis, also during the experiments I received help from several people. I would like to thank Henk van de Bovenkamp for building the setup and arranging materials for the measurements. I also would like to thank the teaching assistants on the lab, Laetitia Vicari, Olga Yevheyuk and Karlijn Meerman. Thank you for your assistance, interest, and advice during the lab days. Additionally, I would like to acknowledge Niek Eisink and Ranjita Bose for coordinating the Bachelor research project. Finally, I also thank my fellow students for their help in the lab.

Bibliography

Dortmund Data Bank (DDB). (n.d.). *Partial pressure methanol*. Http://Ddbonline.Ddbst.de/AntoineCalculation/AntoineCalculationCGI.Exe?Component=Methanol.

He, S., Zuur, K., Santosa, D. S., Heeres, A., Liu, C., Pidko, E., & Heeres, H. J. (2021). Catalytic conversion of pure glycerol over an un-modified H-ZSM-5 zeolite to bio-based aromatics. *Applied Catalysis B: Environmental*, *281*. https://doi.org/10.1016/j.apcatb.2020.119467

Li, H., Li, X. G., & Xiao, W. de. (2021). Collaborative Effect of Zinc and Phosphorus on the Modified HZSM-5 Zeolites in the Conversion of Methanol to Aromatics. *Catalysis Letters*, *151*(4), 955–965. https://doi.org/10.1007/s10562-020-03360-3

Niu, X., Wang, K., Bai, Y., Du, Y. E., Chen, Y., Dong, M., & Fan, W. (2020). Selective formation of para-xylene by methanol aromatization over phosphorous modified ZSM-5 zeolites. *Catalysts*, *10*(5). https://doi.org/10.3390/catal10050484

Olsbye, U., Svelle, S., Bjrgen, M., Beato, P., Janssens, T. V. W., Joensen, F., Bordiga, S., & Lillerud, K. P. (2012). Conversion of methanol to hydrocarbons: How zeolite cavity and pore size controls product selectivity. In *Angewandte Chemie - International Edition* (Vol. 51, Issue 24, pp. 5810–5831). https://doi.org/10.1002/anie.201103657

Pinilla-Herrero, I., Borfecchia, E., Holzinger, J., Mentzel, U. v., Joensen, F., Lomachenko, K. A., Bordiga, S., Lamberti, C., Berlier, G., Olsbye, U., Svelle, S., Skibsted, J., & Beato, P. (2018). High Zn/Al ratios enhance dehydrogenation vs hydrogen transfer reactions of Zn-ZSM-5 catalytic systems in methanol conversion to aromatics. *Journal of Catalysis*, *362*, 146–163. https://doi.org/10.1016/j.jcat.2018.03.032

Rouquerol, J. ; A. D. ; F. C. W. ; E. D. H. ; H. J. M. ; P. N. ; R. J. D. F. ; S. K. S. W. ; U. K. K. (1994). Recommendations for the characterization of porous solids (Technical Report). *Pure and Applied Chemistry*, *66*(8), 1739–1758. https://doi.org/10.1351/pac199466081739

Shoinkhorova, T., Cordero-Lanzac, T., Ramirez, A., Chung, S. H., Dokania, A., Ruiz-Martinez, J., & Gascon, J. (2021). Highly selective and stable production of aromatics via high-pressure methanol conversion. *ACS Catalysis*, *11*(6), 3602–3613. https://doi.org/10.1021/acscatal.0c05133

Sietsma, J. R. A., Jos Van Dillen, A., de Jongh, P. E., & de Jong, K. P. (2006). *Application of ordered mesoporous materials as model supports to study catalyst preparation by impregnation and drying*.

Sing, K. S. W. (1982). Reporting physisorption data for gas/solid systems. *Pure and Applied Chemistry*, *54*(11), 2201–2218. https://doi.org/10.1351/pac198254112201

Structure Commission of the International Zeolite Association (IZA-SC). (2017). *Database of Zeolite Structures*. https://asia.iza-structure.org/IZA-SC/pow_pat.php?STC=MFI&ID=MFI_1

Wan, Z., Li, G., Wang, C., Yang, H., & Zhang, D. (2018). Effect of Reaction Conditions on Methanol to Gasoline Conversion over Nanocrystal ZSM-5 Zeolite. *Catalysis Today*, *314*, 107–113. https://doi.org/10.1016/j.cattod.2018.01.017

Winkelman, J. G. M. (2020). *Reader CHTT-09 Technical Thermodynamics 2019 2020 20191203*.

Zhang, J., Qian, W., Kong, C., & Wei, F. (2015). Increasing para-Xylene Selectivity in Making Aromatics from Methanol with a Surface-Modified Zn/P/ZSM-5 Catalyst. *ACS Catalysis*, *5*(5), 2982–2988. https://doi.org/10.1021/acscatal.5b00192

Zhao, W., Zhang, B., Wang, G., & Guo, H. (2014). Methane formation route in the conversion of methanol to hydrocarbons. *Journal of Energy Chemistry*, *23*(2), 201–206. https://doi.org/10.1016/S2095-4956(14)60136-4

Zhu, X., Zhang, J., Cheng, M., Wang, G., Yu, M., & Li, C. (2019). Methanol Aromatization over Mg-P-Modified [Zn,Al]ZSM-5 Zeolites for Efficient Coproduction of para-Xylene and Light Olefins. *Industrial and Engineering Chemistry Research*, *58*(42), 19446–19455. https://doi.org/10.1021/acs.iecr.9b03743

Appendix

Appendix A: Derivation WHSV calculations

$$P_{MeOH} = 354\ mbar$$

$$P_{total} = 1000\ mbar$$

$$F_{N2} = 41\ mL/min$$

$$F_{total} = F_{MeOH} + F_{N2}$$

$$F_{MeOH} = x\ mL/min$$

$$F_{total} = x + 41\ mL/min$$

$$P_{total} = P_{MeOH} + P_{N2} = 1\ bar$$

$$\frac{F_{MeOH}}{F_{total}} = \frac{P_{MeOH}}{P_{total}}$$

$$\frac{x}{x + 41} = \frac{354}{1000}$$

$$x = 0.354(x + 41)$$

$$0.646x = 14.514$$

$$x = 22.467\ mL/min$$

$$F_{MeOH} = 22.467\ mL/min$$

$$F_{total} = 22.467 + 41 = 63.467\ mL/min$$

$$PV = nRT$$

$$n = \frac{VP}{RT} = \frac{22.467 * 10^{-6} * 10^{5}}{8.314 * 298} = 9.068 * 10^{-4}\ mol/min$$

$$F_{mass,MeOH} = 9.068 * 10^{-4} * 32.04 = 0.02904\ g/min$$

$$F_{mass,MeOH} = 1.74\ g/hr$$

$$WHSV = \frac{F_{mass,MeOH}}{M_{catalyst}} = \frac{1.74}{0.200} = 8.7\ hr^{-1}$$

Appendix B: Piping and instrumentation diagram (P&ID)

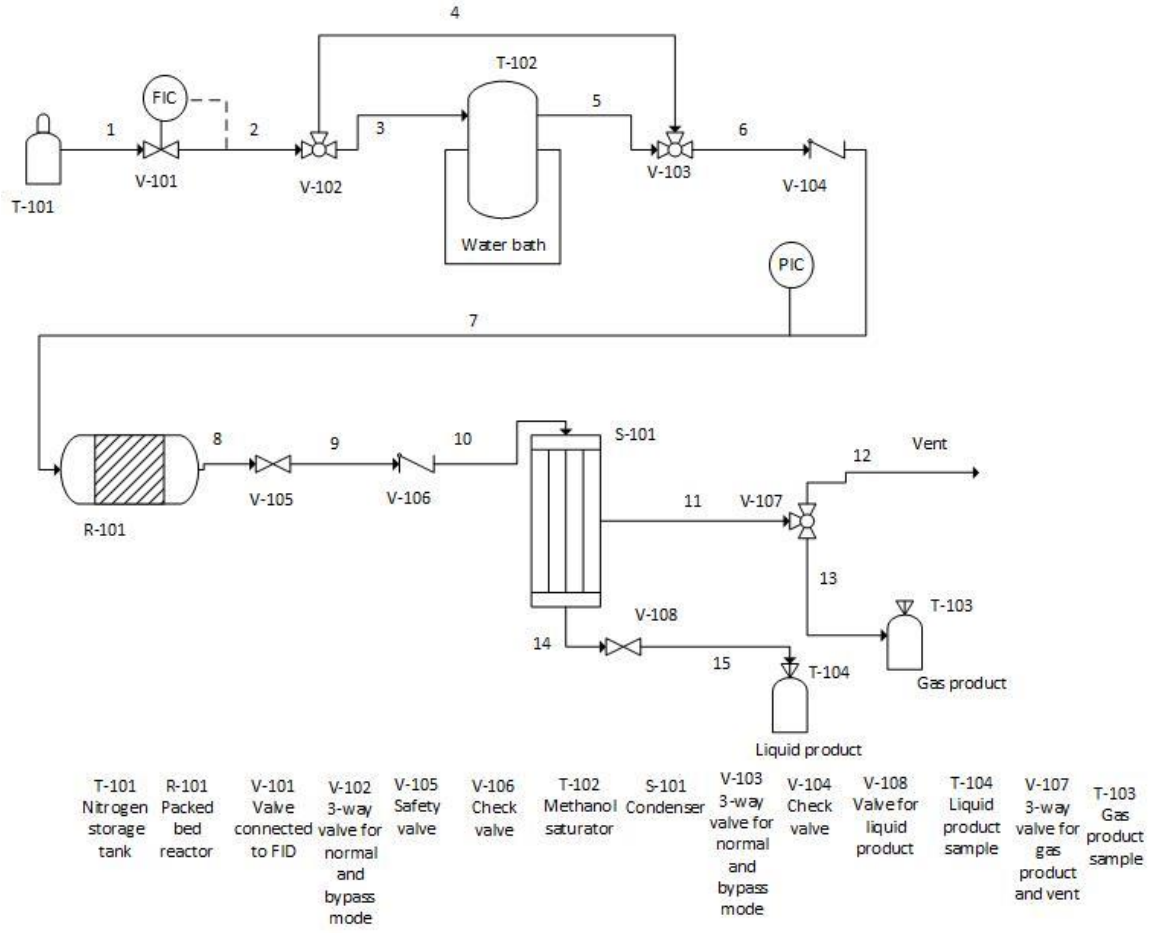

Appendix C: Hazard and Operability study (HAZOP)

No.	Deviation	Possible causes	Consequences	Action required
1	No N_2-flow	N_2-tank valve is closed	No reaction occurs	Check before experiment if N_2 tank valve is open. Also check the flow meter.
2	Less N_2-flow	Leakage Wrong value set to flow meter	Less methanol is transported to the reactor	Check for leakages at N_2 tank. Check if setting on flow meter are right
3	More N_2-flow	Wrong value set to flow meter N_2-flow pressure is too high	Methanol in absorber is splashing around, too much methanol is transported to reactor	Lower the setting on the flow meter. Lower the pressure at N_2 tank (around 2 bar)
4	Higher temperature heater of reactor	Wrong settings heater	T >550°C reactor melts	Lower temperature of heater
5	Lower temperature	Wrong settings heater	Wrong reaction conditions	Increase temperature of heater

	heater of reactor			
6	Before reaction valves are in “normal” mode	Wrong positioning of valves	Methanol absorber cycle is not blocked (methanol is transported to reactor before reaction should start)	Change position of the vales to the “bypass” mode
7	Higher temperature of methanol saturator	Heater is at a too high value	The saturation of methanol in the N_2-stream is too high	Set the heater of the methanol saturator to the right temperature
8	Lower temperature of methanol saturator	Heater is at a too low value	The saturation of methanol in the N_2-stream is too low	Set the heater of the methanol saturator to the right temperature
9	Safety valve closed	Pressure increase	Breaking of glassware, especially at glas-glas surfaces	Open safety valve
10	Lower pressure	Leakage	No pressure gradient in system	Find leakage with “leakage test”. First check if methanol in the saturator bubbles when “normal mode” of the valves is used. If this is the case, there is no leakage in the methanol saturator cycle. Then go back to “bypass” mode and close safety valve. Set the flow meter to ~8 ml/hr and check if the pressure keeps constant. If this is the case, there is no leakage in the part between the methanol saturator and the safety valve. If the pressure equals 0, there is a leakage, because the pressure in the system is the same as outside the system. This means that there is no overpressure
11	Higher pressure	Blockage	Breaking of glassware	Set the N_2-flow to zero and stop heating. Try to find where the blockage is located and remove the blockage.
12	Vent valve is closed	Vale is not opened again after a gas sample was taken	Too high pressure. Glassware could break	Open the vent valve, this valve is always open. Only when taking gas samples this valve is closed.
13	Gas flows back to the reactor or	Check valve is broken	No gas comes out the outlet streams.	Remove the broken check valve and replace the old valve

	back to the methanol saturator (wrong direction)		High gas flow stream in the methanol saturator	
14	Methanol bubbles under “bypass” mode	Valves for “normal” and “bypass” mode are broken	Methanol is transported to the reactor while this should not be the case	Replace the valves
15	Gas comes out vent stream or product stream while safety valve is closed	Safety valve is broken	The safety valve does not stop the gas flow to the condenser	Replace the valve
16	No cooling of condenser	Cooler is set to wrong temperature Condenser is broken Cooling water flow is too low	No liquid product because the components are not condensed	Check if the temperature controller is at the right temperature. Also check if the cooling water stream and the cooler itself is on. If this is all the case condenser or cooler is broken and has to be removed